# ASSESSMENT OF SEMI-MECHANISTIC BUBBLE DEPARTURE DIAMETER MODELLING FOR THE CFD SIMULATION OF BOILING FLOWS

**Marco Colombo[1], Ronak Thakrar[2], Michael Fairweather[1] and Simon P. Walker[2]**
[1] School of Chemical and Process Engineering
University of Leeds, Leeds, LS2 9JT, United Kingdom
[2] Department of Mechanical Engineering, Imperial College London,
Exhibition Road, London, SW7 2AZ, United Kingdom

## ABSTRACT

In Eulerian-Eulerian two-fluid computational fluid dynamic (CFD) models, increasingly often applied to the prediction of nucleate boiling in nuclear reactor thermal hydraulics, boiling at the wall is usually accounted for by partitioning the heat flux between the different mechanisms of heat transfer involved. Between the numerous closures required, the bubble departure diameter in particular has a significant influence on the predicted interfacial area concentration and void distribution within the flow. In the present work, and following evidence of the limited accuracy and reliability of the empirically-based correlations which are applied normally in CFD models, more mechanistic formulations of bubble departure have been introduced into the STAR-CCM+ code. The performance of these models, based on a balance of the hydrodynamic forces acting on a bubble, and their compatibility with existing implementations in a CFD framework, are assessed against two different data sets for vertically upward subcooled boiling flows. In general, a significant amount of modelling is required by these mechanistic models and some recommendations are made on different modelling choices. The model is extended to include a more physically-consistent coupled calculation of the frequency of bubble departure and the modelling of the local subcooling acting on the bubble cap is analyzed. In general, predictions of void distribution and wall temperature reach a satisfactory accuracy, even if numerous numerical and modelling uncertainties are still present. In view of this, several areas for future work and modelling improvement are identified.

**KEYWORDS**
Nucleate boiling, computational fluid dynamics, bubble departure diameter, semi-mechanistic model

## 1. INTRODUCTION

In the nuclear industry, practically all water-cooled nuclear reactors experience some degree of boiling, during normal operation as well as in design-basis and beyond design-basis postulated accident scenarios. In recent years, many attempts have been made to incorporate wall boiling models into computational fluid dynamic (CFD) codes, and most commercial CFD platforms now include some boiling capability inside their two-fluid averaged models. The development of these CFD approaches, which are inevitably used when addressing industrial-scale engineering problems, has proved of value in the prediction of multiphase flows. More specifically, the possibility to capture physical processes across the length scales in greater detail with respect to conventional thermal hydraulic approaches makes CFD appealing for multiphase nuclear reactor thermal hydraulics and the prediction of phenomena such as boiling and the critical heat flux, for which robust and reliable modelling is still not available [1, 2].

In the majority of CFD codes, wall boiling capability is typically based on the Rensselaer Polytechnic Institute (RPI) heat flux partitioning model introduced by Kurul and Podowski [3]. In this model, the heat flux from the wall is partitioned between the mechanisms that are presumed to be responsible for the heat

transfer process, assumed to be single-phase convection, quenching and evaporation. Although the RPI model and all its more recent modifications are structured in a mechanistic fashion, they have been forced to rely on numerous mostly empirical or semi-empirical closure relations. The evaporative heat transfer component, for instance, requires closure relations for the active nucleation site density, the bubble departure diameter and the bubble departure frequency. In most CFD studies to date, these have been predicted with different empirical correlations, which have been reviewed in [4] and [5]. The wider applicability of the RPI model is thus limited and calibration has been often required to accurately predict the data set under investigation [6-8]. It is therefore expected that the predictive capability of the RPI model might be improved by gradually replacing current mostly empirical sub-modelling in favour of more mechanistic sub-modelling.

This paper investigates semi-mechanistic modelling of the bubble departure diameter closure relation. In the RPI model, the value of the departure diameter is required to calculate the evaporative heat flux and the surface area of interest in the boiling process. In addition, the bubble departure diameter determines the wall nucleation contribution in population balance models that are often included in the two-fluid framework to track the evolution of the bubble diameter distribution in the flow. Therefore, accuracy of this particular closure has a strong impact upon predicted mean flow quantities, including the void fraction distribution and the temperature field in the liquid.

Numerous semi-mechanistic approaches for predicting the departure diameter under forced convective conditions have been proposed in recent decades. These originate from the models of Klausner et al. [9], in which bubble growth is computed from a growth rate model and a balance of several local hydrodynamic forces on the bubble determines the diameter at the moment of detachment from the nucleation cavity. Over the years, subsequent modelling efforts have largely attempted to calibrate Klausner's model to extend predictive capability towards a wider range of experimental conditions. Yun et al. [10] introduced the effect of local condensation into the bubble growth rate model and suggested modifications to both the lift force and the surface tension models. Sugrue and Buongiorno [11] calibrated Klausner's model against several low-pressure data sets by making adjustments to the contact diameter model. Whilst these models continue to incorporate a heavy empirical component, it is hoped nevertheless that the more local considerations involved will extrapolate more effectively toward high-pressure pressurized water reactor (PWR) conditions, where measurements of diameter are scarce for obvious reasons. Recently, Colombo and Fairweather [12] extended Yun's model by including the contribution of microlayer evaporation beneath the bubble.

Overall, these models have been rarely implemented inside CFD codes [10, 13]. Even less frequent have been analyses focused on the force-balance model itself, particularly in relation to the local near-wall flow conditions that are required as input, normally at a length scale smaller than the first near-wall finite-volume cell, in particular at high pressure. To the best of the author's knowledge, the only exception to this is the recent work of Thakrar and Walker [14], who undertook an examination of the implementation of the force-balance model of Sugrue and Buongiorno [11] in the STAR-CCM+ commercial code [15] against the popular high pressure subcooled boiling test case of Bartolomei and Chanturiya [16]. Instead, the bubble departure diameter has most often been obtained from empirical correlations. Amongst numerous options, correlations from Tolubinsky and Kostanchuk [17] and Kocamustafaogullari [18] are frequently used. Being derived from mean parametric data, these are not, however, equipped to reflect the dependency on the local flow conditions that are normally available in a CFD calculation [14].

In this work, three force balance models, from Klausner et al. [9], Yun et al. [10] and Sugrue and Buongiorno [11], are implemented in the STAR-CCM+ code [15]. The performance of the CFD model is assessed blindly against the experiments of Bartolomei and Chanturiya [16] and Garnier et al. [19] (referred to more commonly as the DEBORA benchmark) for subcooled boiling flows of water and refrigerant in vertical pipes. Results are also compared with the most frequently used empirical

correlations. Impacts on the results of different modelling choices are examined and results of the force balance analyzed and possible improvements in the modelling of some forces suggested. Bubble departure frequency is also directly evaluated from the force balance model, improving the internal physical consistency of the model. Finally, some sensitivity studies are made on the modelling of condensation on the bubble cap.

## 2. EXPERIMENTAL DATA

Two experiments from the database of Bartolomei and Chanturiya [16] and the DEBORA experiment [19] have been predicted in this work, with the specific conditions of these being reported in Table I.

**Table I. Experimental conditions of the two test cases.**

| Experiment | p [MPa] | G [kg $m^{-2}s^{-1}$] | q [$kWm^{-2}$] | $T_{in}$ [˚C] | D [m] | Fluid |
|---|---|---|---|---|---|---|
| **Bartolomei** | 4.5 | 900 | 570 | 197.4 | 0.0154 | Water |
| **DEBORA** | 2.62 | 1985 | 73.9 | 70.5 | 0.0192 | R12 |

Bartolomei and Chanturiya [16] investigated the subcooled boiling of water flowing upward in a vertical pipe of inner diameter $D$ = 0.0154 m and length $L$ = 2 m. Area-averaged void fractions were measured using a gamma-ray attenuation technique driven by a Thulium-170 source at different axial locations and at pressures up to 15 MPa, mass fluxes up to 2000 kg $m^{-2}$ $s^{-1}$ and heat fluxes up to 2.2 MW $m^{-2}$. In addition, wall temperature, axial liquid temperature and area-averaged liquid temperature measurements were also provided at 4.5 MPa, and, therefore, this specific experiment is simulated here.

The DEBORA [19] flow loop consisted of a 19.2 mm inner diameter vertical pipe, heated for a length of 3.5 m and operated with Freon-12 (R-12). It is both difficult and expensive to measure the flow boiling behaviour of water at high pressure. Employing R-12 as the working fluid partially replicates the flow characteristics of a prototypical high pressure flow of water under much milder conditions. In the range of pressures investigated in the DEBORA experiment (1.46 – 3.01 MPa), the values of the relevant dimensionless groups for R-12, such as the Reynolds and Weber numbers, and the density ratio, are comparable to those found in PWRs. Void fraction and vapour velocity profiles at the end of the test section were measured with an optical probe technique, from which radial profiles of the interfacial area concentration and the Sauter mean diameter (SMD) were determined. Thermocouples were used to measure the liquid temperature radial profile and the wall temperature at selected axial locations. Details of the specific experiment investigated here, characterized by a pressure of 2.62 MPa, are given in Table I.

Measurements of the bubble departure diameter are not provided by either of the two experiments. Such measurements, particularly under forced convective conditions, are understandably quite scarce at elevated pressure. Similarly, data for mean flow quantities under prototypic reactor operating conditions (~ 15 MPa) is equally scarce. The two databases selected are amongst the most frequently employed for validating CFD boiling capability, and represent an appropriate compromise between data availability and proximity to true nuclear reactor operating conditions.

## 3. MATHEMATICAL MODEL

In a two-fluid Eulerian-Eulerian model, each phase is described by a set of time averaged conservation equations, and the continuity, momentum and energy equations are solved for each phase. These, being discussed for adiabatic two-phase boiling flows in many previous publications such as [20] to which the interested reader may refer to, are not presented here. Instead, this section is focused on the wall boiling and the bubble departure diameter models, these being the main subject of the work. Implementation of

all the other models follows a standard approach which will be only briefly summarized. A full description of the models as well as the values of the many modelling parameters employed can be found in [15]. The drag model of Tomiyama et al. [21] is used with the model of Burns et al. [22] for the turbulent dispersion. Lift and wall lubrication forces are not included. Although both might affect boiling modelling, their role and magnitude in boiling flows is not well-understood and unlikely to be predicted with accuracy by models designed for adiabatic bubbly flows. A standard high-Reynolds multiphase version of the $k$-$\varepsilon$ turbulence model [23] solves for the turbulence in the liquid phase, whereas in the vapour phase the turbulence is directly related to that in the liquid using a turbulence response model.

Bubbles, after their departure from the heated wall, experience evaporation and condensation in the bulk of the flow, and break-up and coalescence events that alter the bubble diameter distribution and affect the interphase mass, momentum and energy exchanges. The bubble diameter distribution is predicted with the $S_\gamma$ model [24]. Moments of the bubble diameter distribution, which is assumed to obey to a pre-defined log-normal shape, are calculated and used to define the SMD in the flow. The one-equation version of the model is considered, which is described in more detail in [15], with source terms for breakup and coalescence defined following [25], where they were successfully validated against air-water bubbly flows. Here, a value of 1.24 is used for the critical Weber number $We_{cr}$. Finally, condensation and evaporation in the bulk of the fluid are evaluated from the Ranz and Marshall correlation [26].

### 3.1 Wall Heat Flux Partitioning Model

When nucleate boiling takes place at the wall, wall superheat and the related heat transfer coefficient, and the temperature in the wall-adjacent finite-volume cell, are obtained from the solution of the wall heat flux partitioning model. Following the RPI approach, the total heat flux is partitioned between the mechanisms responsible for heat removal:

$$q_w = \left(q_l + q_q + q_{ev}\right)\left(1 - K_{dry}\right) + K_{dry} q_v \tag{1}$$

Latent heat is removed by evaporation ($q_{ev}$) and supports the growth of vapour bubbles at the active nucleation sites. Detachment of these bubbles promotes additional mixing by drawing in cooler liquid in the space previously occupied by the bubble, causing rewetting of the heating surface, and this additional contribution to the total heat transfer ($q_q$) is often referred to as quenching. In regions of the wall not affected by boiling, sensible heat is transferred to the liquid-phase by ordinary single-phase convection ($q_l$). Finally, if the amount of vapour generated at the wall is high enough so as to begin to obstruct surface rewetting, a portion of the wall heat is transferred by convection to the vapour phase ($q_v$). In this case, the fraction of the wall surface in contact with the vapour phase is represented by $K_{dry}$, which becomes larger than zero when the void fraction is higher than a critical value, assumed equal to 0.9. The heat flux for the single-phase convective contribution is evaluated using standard wall treatments and using the temperature in the near-wall cell $T_l$, as illustrated below:

$$q_l = (1 - A_b) h_l (T_w - T_l) = (1 - A_b) \frac{\rho_l C_{p,l} u_{\tau,l}}{T_l^+} (T_w - T_l) \tag{2}$$

The boiling area fraction $A_b$ is the fraction of the wall affected by the evaporation process and $T_l^+$ is the dimensionless temperature in the near-wall cell. The convective heat flux to the vapour phase is calculated in a similar way. The quenching heat flux is expressed as the product of a quenching heat transfer coefficient, modelled as a transient conduction into a semi-infinite medium, and the temperature difference between the wall and the liquid:

$$q_q = A_b h_q (T_w - T_l) = 2A_b f \sqrt{\frac{\rho_l C_{p,l} \lambda_l t_w}{\pi}} (T_w - T_l) \quad (3)$$

In the previous equation, the waiting time $t_w$ is equal to 80 % of the total ebullition cycle of a bubble, known from the inverse of the bubble departure frequency $f$, and, to avoid any dependency on the computational grid, the liquid temperature is evaluated at a constant wall $y^+$ of 250. The evaporative heat flux is known from the mass flux of bubbles generated at the wall and the latent heat of vaporization $i_{lv}$. Assuming the bubbles are spherical, this mass flux is easily computed from the number of nucleation sites active per unit area $N_A$, the bubble departure diameter $d_b$ and the bubble departure frequency $f$:

$$q_{ev} = N_A f \left(\frac{\pi d_b^3}{6}\right) \rho_v i_{lv} \quad (4)$$

The nucleation site density and bubble departure diameter are also used to derive the fraction of the wall exposed to the boiling process:

$$A_b = 2.0 \frac{\pi d_b^2}{4} N_A \quad (5)$$

In view of the modelling presented, it is clear that predictions of the heat flux partitioning model are strongly related to the closure models for the active nucleation site density, the bubble departure diameter and the bubble departure frequency. Normally, these are predicted using empirical closures that, being mostly derived from bulk parameters, show limited accuracy and applicability, and solutions that are frequently grid-dependent. Correlations for the active nucleation site density in particular are associated with significant uncertainty related to the specific conditions of the surface. This is not addressed in the present paper and the site density is predicted using the correlation of Hibiki and Ishii [27], which has been shown to give a ~ 50% error for high pressure water flows.

The bubble departure diameter is calculated from a force balance approach. More specifically, bubble growth is predicted from an energy balance that accounts for the different mechanisms of heat transfer between the bubble and the wall, and the surrounding liquid. The departure condition is evaluated from balances of the forces acting on the bubble parallel ($x$) and perpendicular ($y$) to the heated wall. Depending on the balance that is violated first, therefore, the departure diameter that is utilised by the heat flux partitioning model describes the diameter at which the bubble departs (parallel) and begins to slide away from the nucleation site and along the wall or lifts-off (perpendicular), moving away from the wall and toward the bulk. The much greater heat fluxes required to drive boiling at elevated pressures cause bubbles to lift-off very quickly [14]. It is thus reasonable to assume that bubbles lift-off immediately following departure at the investigated conditions.

The three force balance models from Klausner et al. [9], Yun et al. [10] and Sugrue and Buongiorno [11] were applied. As discussed previously, the latter two are extensions of the former, which was developed and validated against flow boiling of R113 in a square duct at atmospheric pressure. The balance considers several forces, including a surface tension force $F_{stx/sty}$, a buoyancy force $F_b$, a quasi-steady drag force $F_{qs}$, an unsteady drag force due to asymmetrical bubble growth $F_{dux/duy}$, a shear lift force $F_{sl}$, a hydrodynamic force $F_p$ and a contact pressure force $F_{cp}$. No additional modifications to these forces have been introduced, although their applicability to the investigated conditions is still unclear and, inevitably, the modelling still relies on a number of empirical parameters. The forces and the modifications adopted

are summarized in Table II. For both the Klausner et al. [9] and Sugrue and Buongiorno [11] models, the bubble growth equation from Forster and Zuber [28] with a value of $b$ = 1.56 is used, this being the asymptotic solution of the Mikic et al. [29] model that was originally adopted by Klausner at al. [9]. A similar modification was introduced in a subsequent paper from the same research group [30]. Yun et al. [10] added the contribution of the locally subcooled flow and the condensation heat transfer coefficient was evaluated using the Ranz and Marshall correlation [26]. These models are compared with the widely applied correlations of Tolubinsky and Konstanchuk [17] and Kocamustafaogullari [18], which are also summarised in Table II.

**Table II. Summary of the model for bubble departure diameter and bubble departure frequency.**

| **Model** | **Form** |
|---|---|
| Force balance | $\sum F_x = F_{stx} + F_{qsd} + F_b \sin\theta + F_{dux} = 0$<br>$\sum F_y = F_{sty} + F_{sl} + F_b \cos\theta + F_{duy} + F_p + F_{cp} = 0$<br>$F_{stx} = -1.25 d_w \sigma \frac{\pi(\alpha-\beta)}{\pi^2-(\alpha-\beta)^2}(\sin\alpha - \sin\beta)$<br>$F_{sty} = -d_w \sigma \frac{\pi}{(\alpha-\beta)}(\cos\beta - \cos\alpha)$<br>$F_{qsd} = 6\pi\rho_l \nu U R \left\{\frac{2}{3} + \left[\left(\frac{12}{Re}\right)^{0.65} + 0.862\right]^{-1.54}\right\}$<br>$F_{du} = -\rho_l \pi R^2 \left(\frac{3}{2}\dot{R}^2 - R\ddot{R}^2\right)$<br>$F_b = \frac{4}{3}\pi R^3(\rho_l - \rho_v)g$<br>$F_{sl} = \frac{1}{2}\pi\rho_l U^2 R^2 \{3.877 G_s^{0.5}[Re^{-2} + (C_l G_s^{0.5})^4]^{0.25}\}$<br>$F_p = \frac{9}{8}\rho_l U^2 \frac{\pi d_w^2}{4}$<br>$F_{cp} = \frac{\sigma}{R}\frac{\pi d_w^2}{4}$<br>$\frac{dR(t)}{dt} = \frac{2b}{\sqrt{\pi}} Ja \sqrt{a t_w}; b = 1.56$ |
| Klausner et al. [9] | $d_w = 0.09$ mm $\quad C_l = 0.014$ |
| Sugrue and Buongiorno [11] | $d_w/d_b = 0.025 \quad C_l = 0.014$ |
| Yun et al. [10] | $d_w/d_b = 0.067 \quad C_l = 0.118$<br>$\frac{dR(t)}{dt} = \frac{2b}{\sqrt{\pi}} Ja \sqrt{a t_w} - \frac{b q_c}{S h_{lv} \rho_v} t_w; b = 1.56; S = 2$ |
| Tolubinsky and Kostanchuk [17] | $d_w = d_0 exp[-(T_{sat} - T_l)/\Delta T_0]$ |
| Kocamustafaogullari [18] | $d_w = d_l \theta \left(\frac{\sigma}{g\Delta\rho}\right)^{0.5} \left(\frac{\Delta\rho}{\rho_v}\right)^{0.9}$ |
| Cole [31] | $f = \sqrt{\frac{4}{3}\frac{g(\rho_l - \rho_v)}{d_w \rho_l}}$ |
| Waiting time | $t_w = 0.8/f$ |

Initially, the bubble departure frequency was calculated from the correlation of Cole [31]. However, the force balance model assumes a growth rate equation, and the growth time that is derived from this may contradict the value of the departure frequency predicted using Cole's correlation. In this work, the departure frequency is obtained directly from the growth rate equation, with the growth time assumed to make up 20% of the total ebullition period, and the obtained results are then compared against Cole's

correlation. In order to examine the impact of condensation effects, the implementation of the Yun et al. [10] force balance model is undertaken exclusive of the condensation contribution in the growth rate equation in the first instance. It is worth remarking that the authors do not describe how the liquid temperature used in their growth rate equation is determined. Whilst this is expected to be the local temperature, indirect evidence suggests that the wall cell temperature was in fact employed. In the interest of remaining consistent with the original form of the model, similar assumptions are employed herein.

### 3.2 Numerical Implementation

The overall model was solved using the steady-state solver of the STAR-CCM+ CFD code [15]. A two-dimensional axisymmetric geometry was employed and, at the inlet, a fully-developed single-phase liquid velocity, turbulence and temperature were imposed, together with an imposed pressure at the outlet and the no-slip condition, and an imposed heat flux, at the wall. Constant thermophysical properties were used for both phases. More specifically, liquid properties were calculated at the average temperature between the inlet and saturation, and matched carefully against the experiment inlet mass flux. Vapour properties were calculated at saturation. A mesh sensitivity study, which is not reported here, demonstrated that grid-independent solutions were achieved with an equidistant structured mesh that ensured the minimum wall $y+$ was greater than 30 (for a total number of grid elements equal to 20 x 375 for Bartolomei and 20 x 750 for DEBORA), therefore sufficiently high to justify the selected high-Reynolds wall treatment.

## 4. RESULTS AND DISCUSSION

The first set of results is shown in Figures 1 and 2 for the two experiments. Predictions from the three force balance models, neglecting subcooling in Yun et al. [10], coupled with the Cole [31] correlation for bubble departure frequency, are compared against wall temperature data, Tolubinsky and Kostanchuk [17] and Kocamustafaogullari [18]. Bubble departure diameter predictions are generally spread over a few orders of magnitude, even if this translates into differences in the wall temperature that are limited to a 10 K range for the data in Figure 1(b) and 5 K for that in Figure 2(b).

Some issues with the Klausner et al. [9] model are immediately observable from Figure 1. At a certain distance from the inlet, a well-defined step is found in both the bubble departure diameter and the wall temperature. Downstream, a solution for the lift-off diameter could not be found and the code fell back to the bubble departure solution instead. In contrast, upstream a solution for the lift-off diameter was successfully computed. This inconsistency is related to the constant contact diameter $d_w$ used in Klausner et al. [9], which, for the specific conditions studied, is sometimes even higher than the bubble diameter and, therefore, prevents the code reaching an acceptable (positive) solution. Even if the same inconsistency is not found in Figure 2, a value of $d_w$ that depends on the bubble diameter, such as those adopted by Sugrue and Buongiorno [11] and Yun et al. [10], is clearly preferable. These models consistently report positive solutions for both force balances. The force balance parallel to the wall is broken first, suggesting that the bubbles may slide first before lifting off. Reasonable agreement with the Bartolomei and Chanturiya [16] experiment is found, except in the final section of the pipe, where a sudden increase in wall temperature is predicted by both Sugrue and Buongiorno [11] and Yun et al. [10]. In the DEBORA experiment [19], the wall temperature is over predicted, although not excessively.

The Kocamustafaogullari [18] correlation predicts values in the neighborhood of the force balance results. A constant value is predicted because the correlation is only a function of pressure, once the fluid properties are assumed constant with temperature. In contrast, Tolubinsky and Kostanchuk [17] returns very high values of the bubble departure diameter and, consequently, under predicts the wall temperature. This was already observed in [14] for the Bartolomei and Chanturiya [16] experiment, and confirmation is found here for the DEBORA experiment [19]. For this reason, Tolubinsky and Kostanchuk [17] is not

used in the following comparisons. In a similar way, and in agreement with the preceding discussion, only the Sugrue and Buongiorno [11] and Yun et al. [10] models are considered below.

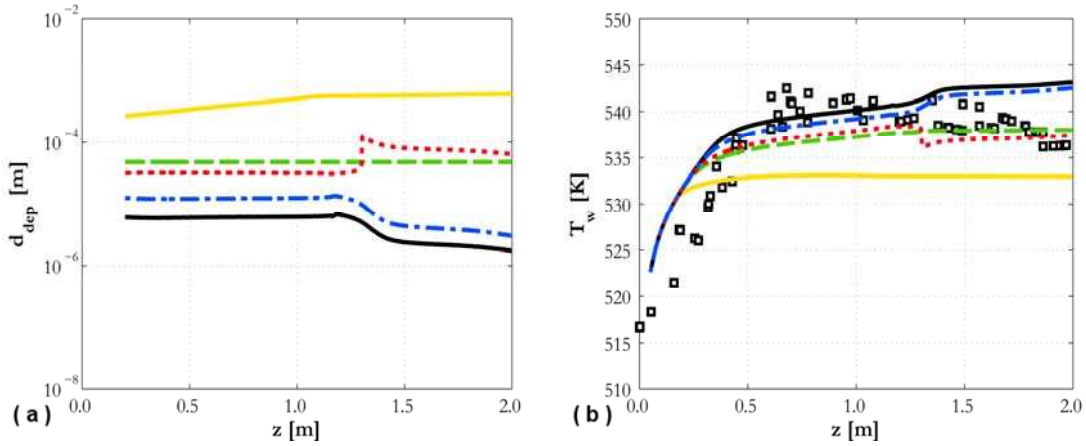


**Figure 1. Predicted bubble departure diameter (a) and wall temperature (b) for Bartolomei and Chanturiya experiment: (□) data; (—) Tolubinsky and Kostanchuk; (– –) Kocamustafaogullari; (··) Klausner et al.; (—) Sugrue and Buongiorno; (– · –) Yun at al. without subcooling. Bubble departure frequency from Cole.**

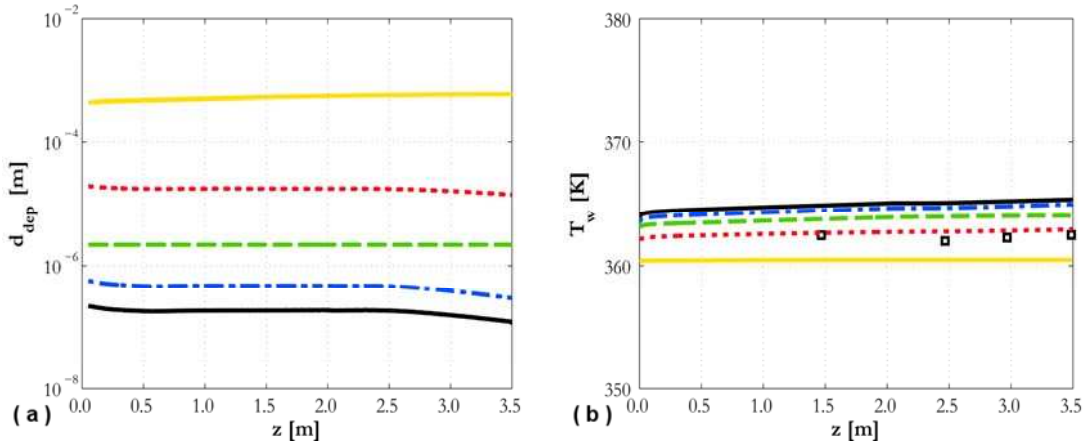


**Figure 2. Predicted bubble departure diameter (a) and wall temperature (b) for DEBORA experiment: (□) data; (—) Tolubinsky and Kostanchuk; (– –) Kocamustafaogullari; (··) Klausner; et al. (—); Sugrue and Buongiorno; (– · –) Yun et al. neglecting subcooling. Bubble departure frequency is calculated from Cole.**

In Figures 1 and 2, the Cole [31] model was used to predict the bubble departure frequency. In Figures 3 and 4, the bubble growth time from the departure routine was used to evaluate the frequency of bubble departure and this is compared against Cole [31], using the Sugrue and Buongiorno [11] bubble departure model. Clearly, using a frequency decoupled from the departure diameter calculation can generate physical inconsistencies in the solution that can overcome the benefits of the more mechanistic bubble departure model. More specifically, near the end of the pipe, the departure diameter decreases (Figure 1(a)) but the frequency from Cole [31] remains almost constant (Figure 3(a)). This, from Eq. (4), reduces the evaporative heat flux, causing the increase in wall temperature observed in Figures 1(b) and 3(b). Using the calculated departure time, a decrease in departure diameter corresponds to a faster growth time and an increase in frequency. Therefore, the evaporative heat flux does not decrease and a flatter temperature profile is found that is more in agreement with the experiments (Figure 3(b)). Similar findings are found for the DEBORA experiment [19] in Figure 4. A reduction in the departure diameter is

reflected in a higher frequency and a wall temperature slightly more in agreement with experiments. Overall, the coupled departure diameter and frequency calculation improves the internal consistency of the model, although the predicted frequency may differ from Cole [31] by up to two orders of magnitude.

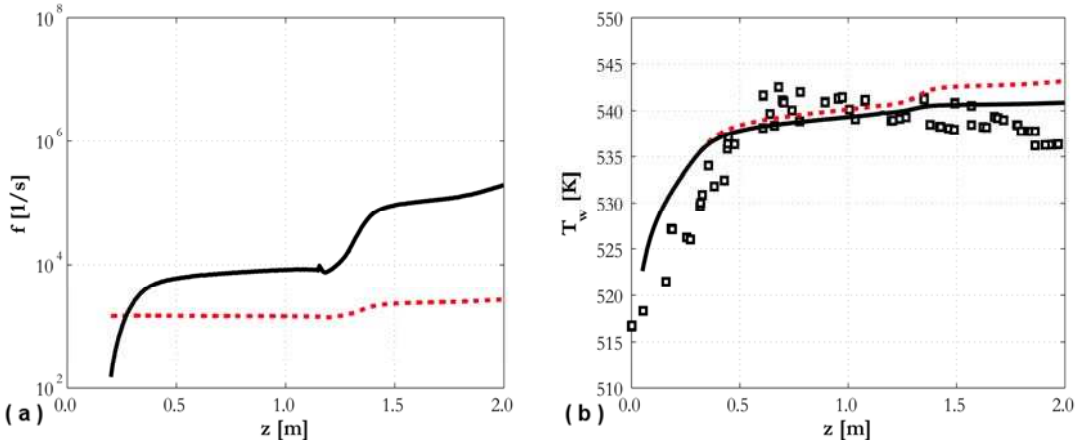


**Figure 3. Predicted bubble departure frequency (a) and wall temperature (b) for Bartolomei and Chanturiya experiment using Sugrue and Buongiorno model: (□) data; (···) Cole model; (—) frequency derived from departure time.**

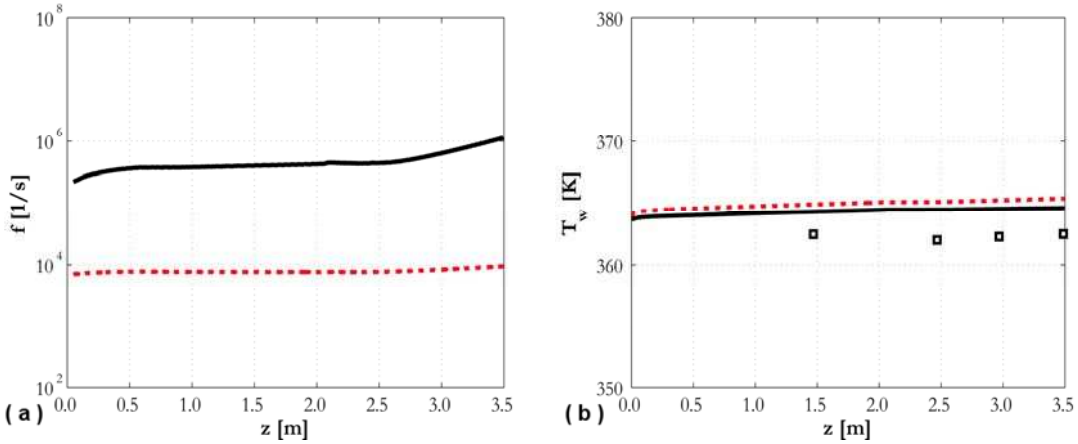


**Figure 4. Predicted bubble departure frequency (a) and wall temperature (b) for DEBORA experiment using Sugrue and Buongiorno model: (□) data; (···) Cole model; (—) frequency derived from departure time.**

Overall comparisons of departure diameter, frequency, wall temperature and evaporative heat flux are reported in Figures 5 and 6. The Sugrue and Buongiorno [11] and Yun et al. [10] models, the latter still neglecting the subcooling contribution, return rather similar predictions, with the latter predicting a higher bubble departure diameter and lower frequency, and slightly lower wall temperature and higher evaporative heat flux. Acceptable agreement is found with wall temperature measurements, even if the observed reduction in wall temperature at the end of the pipe in the Bartolomei and Chanturiya [16] experiment is not reproduced. This is associated indirectly with local flow acceleration in the high void region, and the resulting reduction in predicted diameter under these conditions. Because the partitioning model employed does not consider the effects of coalescence, the trends illustrated are indicative of isolated boiling conditions, and do not reflect the true departure diameter in this region. In the DEBORA experiment [19], the wall temperature is over predicted, although not excessively. No sharp decrease in the force balance predicted departure diameter is observed downstream in the DEBORA experiment, presumably due to the much weaker void prediction in this experiment.

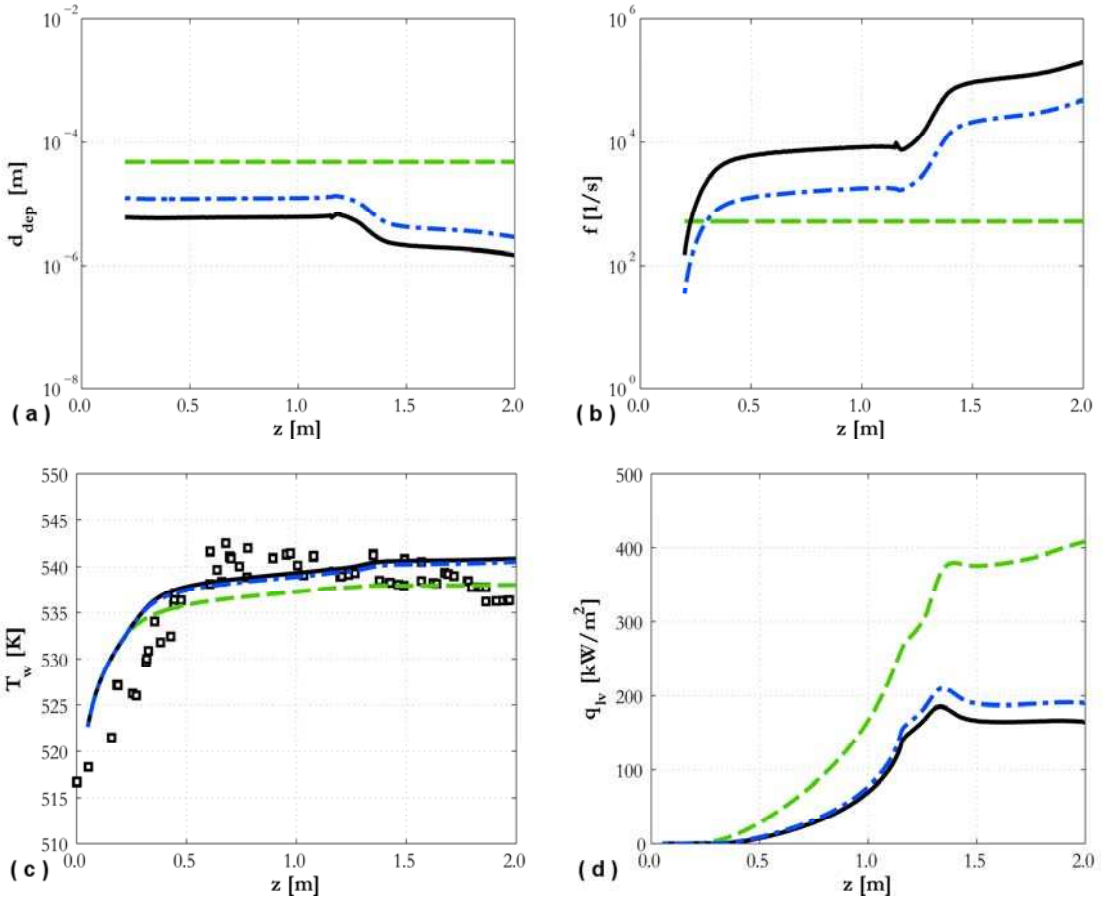


**Figure 5. Predicted bubble departure diameter (a), bubble departure frequency (b), wall temperature (c) and evaporative heat flux (d) for Bartolomei and Chanturiya experiment: (□) data; (– –) Kocamustafaogullari; (—) Sugrue and Buongiorno; (– · –) Yun et al. neglecting subcooling.**

An interesting trend is found in the evaporative heat flux behaviour (Figure 5(d) and 6(d)). Using the Kocamustafaogullari [18] correlation, although the departure diameter and frequency are constant along the pipe, the evaporative heat flux increases in the outlet region, possibly because of an increase in the active nucleation site density. In contrast, the evaporative heat flux is much flatter for the two force balance models. In these, a decrease in departure diameter triggers an increase in frequency. Bubble growth is, however, modelled as only 20% of the total ebullition cycle and, therefore, the contribution of the higher departure frequency to the evaporative contribution is weakened. Therefore, further study in this area and more advanced modelling of the total ebullition cycle would be beneficial.

Details of the magnitude of each force can be found in Figures 7 and 8. In both experiments, the surface tension is the dominant force that keeps bubbles attached to the wall, whereas drag parallel to the wall and shear lift perpendicular to the wall promote bubble departure. Other forces are not expected to be significant, including, at these pressures, gravity. Figures 7 and 8 help to explain some of the behaviour observed previously. The magnitude of the surface tension, which is the dominant negative contribution, depends on the value of the contact diameter $d_w$. From Table II, Yun et al. [10] predicts a higher contact diameter than Sugrue and Buongiorno [11] and, therefore, always a slightly higher bubble departure diameter in Figure 5(a) and 6(a). Klausner at al. [9], in contrast, adopted a constant value that gives results much higher than both of the previous models.

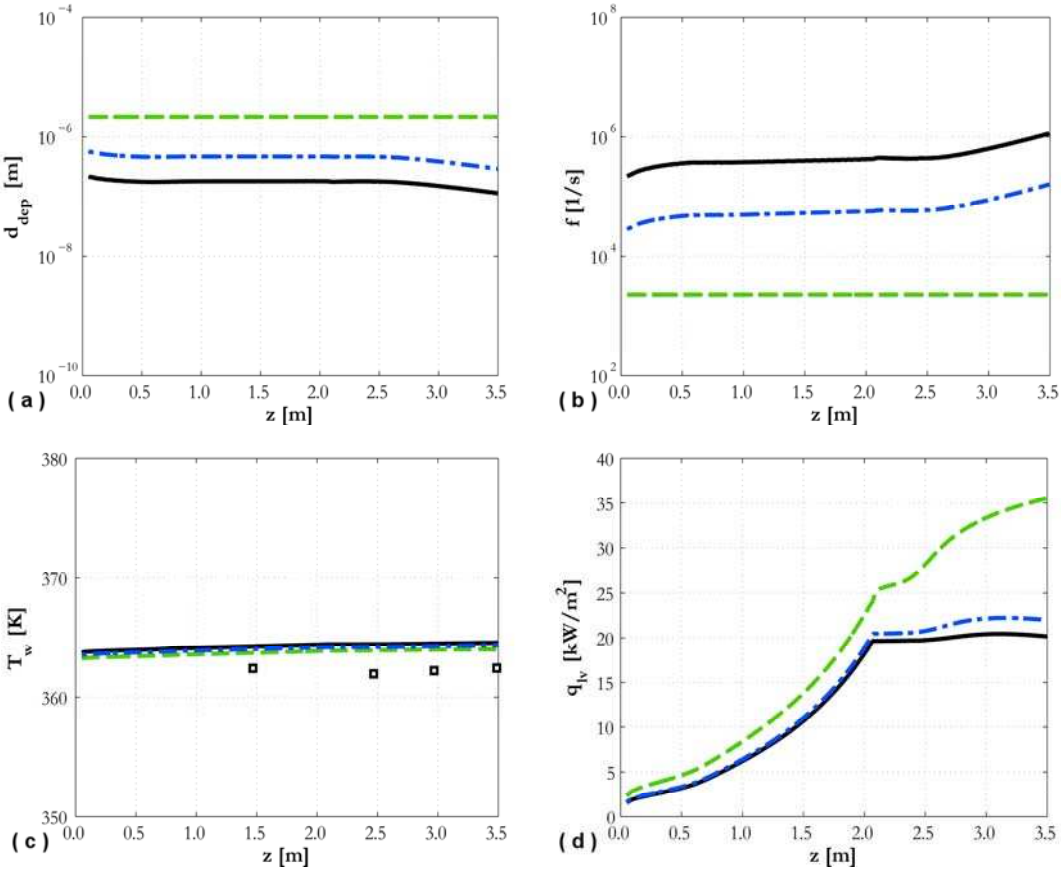


**Figure 6. Predicted bubble departure diameter (a), bubble departure frequency (b), wall temperature (c) and evaporative heat flux (d) for DEBORA experiment: (□) data; (– –) Kocamustafaogullari; (—) Sugrue and Buongiorno; (– · –) Yun et al. neglecting subcooling.**

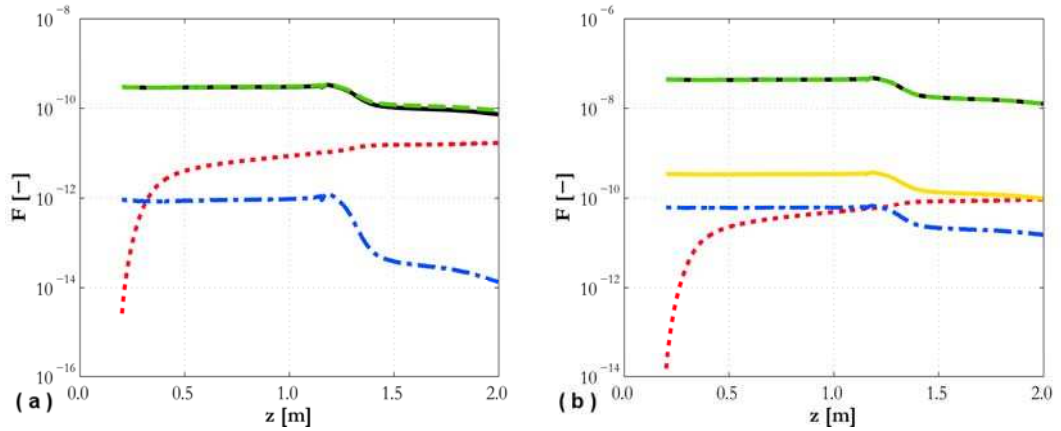


**Figure 7. Contribution to force balance in wall-parallel (a) and wall-normal (b) directions for Bartolomei and Chanturiya experiment: (—) $F_{st}$; (– –) $F_{qsd}$ (a) and $F_{sl}$ (b); (···) $F_{du}$; (– · –) $F_b$ (a) and $F_p$ (b); (—) $F_{cp}$.**

Therefore, and because of the higher surface tension force, when a solution is reached, bubble departure from Klausner et al. [9] is significantly higher than that of Yun et al. [10] and Sugrue and Buongiorno [11]. The latter also both predict a decrease of the departure diameter near the pipe end. An increase in

velocity promoted by boiling is expected to increase the effect of drag and lift, which are the main forces promoting bubble departure. In both cases, the bubble departure balance is violated first with respect to lift-off, therefore bubbles are expected to depart from the nucleation cavity before lifting-off. However, due to uncertainties in the formulation of the drag and lift forces, and in their applicability to the present conditions, additional studies are required.

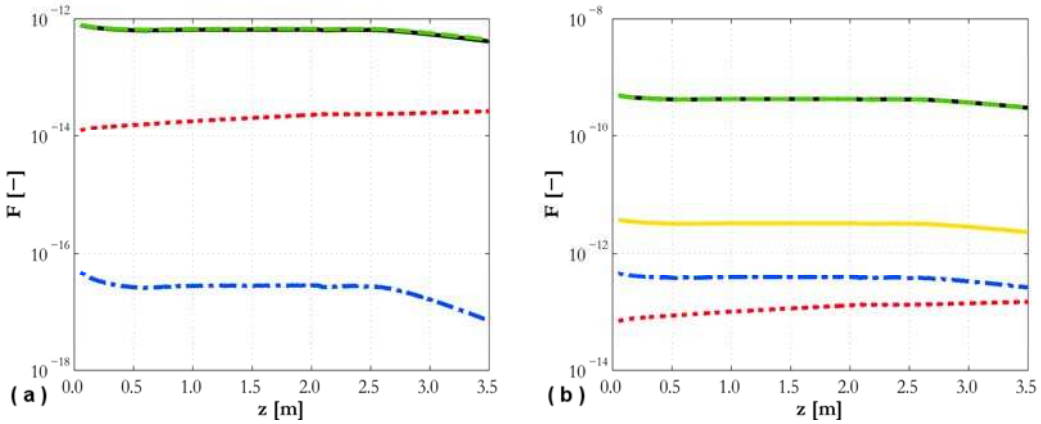


**Figure 8. Contribution to force balance in wall-parallel (a) and wall-normal (b) directions for DEBORA experiment: (—) $F_{st}$; (– –) $F_{qsd}$ (a) and $F_{sl}$ (b); (···) $F_{du}$; (– · –) $F_b$ (a) and $F_p$ (b); (—) $F_{cp}$.**

Preliminary results obtained with subcooling in Yun et al.'s [10] model are considered in Figure 9 which shows the axial wall temperature distribution. In the majority of the region affected by boiling, the temperature in the first cell is superheated. In the first half of the pipe, however, subcooling is significant. Therefore, when the temperature in the first cell is used to evaluate local subcooling, the condensation rate can become so high such that a negative bubble diameter is predicted, thus preventing an acceptable solution from being reached. This is due to the use of temperature in the near-wall cell, which must be located at a certain distance from the wall. In reality, at the pressures of the experiments, the bubbles are much smaller and the temperature in the first cell is not representative of conditions on the bubble cap.

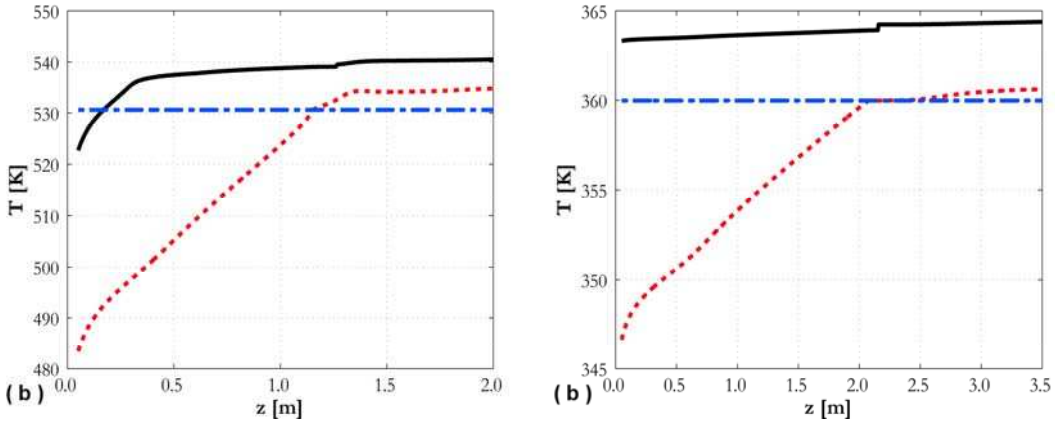


**Figure 9. Predicted temperatures in near-wall region for Bartolomei and Chanturiya (a) and DEBORA (b): (—) wall temperature; (···) liquid temperature in near-wall cell; (– · –) saturation temperature.**

## 5. CONCLUSIONS

Three semi-mechanistic models of bubble departure diameter were implemented into the RPI wall heat flux partitioning model in the STAR-CCM+ code. Model predictions were compared against vertically

upward subcooled boiling flows of water and refrigerant. Limited applicability of the model proposed by Klausner et al. [9], which uses a constant contact diameter in the surface tension force, was demonstrated, and the models of Yun et al. [10] and Sugrue and Buongiorno [11], where the contact diameter is a fraction of the bubble diameter, were shown to be preferable. No clear choice can be made between the two, given that their predictions differ only slightly and are in reasonable agreement with wall temperature measurements. The latter model, however, has the advantage of a more thorough validation. More specifically, Yun et al. [10] validated against the DEBORA experiment, whereas Sugrue and Buongiorno compared against five different databases and a wide range of fluids, geometries and operating conditions. The importance of a coupled calculation of the bubble departure diameter and frequency for improved predictions and better physical consistency of the boiling model was demonstrated. Conversely, the subcooling contribution introduced by Yun at al. [10] predicted excessive condensation, frequently resulting in a negative bubble diameter, because the liquid temperature in the near-wall computational cell was not representative of the local conditions on the bubble cap. Numerous areas of further improvement have been identified. The models predict sliding before lift-off, but the specific magnitude of the surface tension, drag and lift forces, which dominate the force balance, are still uncertain. The general applicability of the models to wall boiling conditions therefore needs to be further investigated. Bubble growth is only a limited part of the whole ebullition cycle and advances in the modelling of this, including the contribution of quenching to the total heat flux, are required for more accurate prediction of the bubble departure frequency. Extension of the model from isolated bubble growth to more sustained boiling conditions, including bubble merging and coalescence during growth, is also of interest. Finally, grid-independent methods to predict real local conditions on the bubble cap are required to account for condensation, and these need to be tested in conditions where condensation is expected to be relevant, such as at lower pressures.

## ACKNOWLEDGMENTS

The authors gratefully acknowledge discussions with Dr. Andrew Splawski and Dr. Simon Lo of CD-adapco and the financial support of the EPSRC, in the framework of the UK-India Civil Nuclear Collaboration, and Rolls-Royce plc.

## REFERENCES

1. D. Bestion, “Applicability of two-phase CFD to nuclear reactor thermalhydraulics and elaboration of best practice guidelines”, *Nuclear Engineering and Design*, **253**, pp. 311-321 (2012).
2. G. Yadigaroglu, “CMFD and the critical-heat-flux grand challenge in nuclear thermal-hydraulics”, *International Journal of Multiphase Flow*, **67**, pp. 3-12 (2014).
3. N. Kurul and M.Z. Podowski, “Multidimensional effects in forced convection subcooled boiling”, *9th International Heat Transfer Conference*, Jerusalem, Israel, 1990.
4. S.C.P. Cheung, S. Vahaji, G.H. Yeoh and J.Y. Tu, “Modelling subcooled flow boiling in vertical channels at low pressure – Part1: assessment of empirical correlations”, *International Journal of Heat and Mass Transfer*, **75**, pp. 736-753 (2014).
5. R. Thakrar, J.S. Murallidharan and S.P. Walker, “An evaluation of the RPI model for the prediction of the wall heat flux partitioning in subcooled boiling flows”, *22nd International Conference on Nuclear Engineering (ICONE 22)*, Prague, Czech Republic, July 7-11, 2014.
6. G.H. Yeoh and J.Y. Tu, “Two-fluid and population balance models for subcooled boiling flow”, *Applied Mathematical Modelling*, **30**, pp. 1370-1391 (2006).
7. E. Krepper, R. Rzehak, C. Lifante and T. Frank, “CFD for subcooled flow boiling: Coupling wall boiling and population balance models”, *Nuclear Engineering and Design*, **255**, 330-346 (2013).
8. M. Colombo and M. Fairweather, “Accuracy of Eulerian-Eulerian, two-fluid CFD boiling models of subcooled boiling flows”, *International Journal of Heat and Mass Transfer*, **103**, 28-44 (2016).

9. J.F. Klaunser, R. Mei, D.M. Bernhard and L.Z Zheng, “Vapor bubble departure in forced convection boiling”, *International Journal of Heat and Mass Transfer*, **36**, pp. 651-662 (1993).
10. B.J. Yun, A. Splawski, S. Lo and C.H. Song, “Prediction of a subcooled boiling flow with advanced two-phase flow models”, *Nuclear Engineering and Design*, **253**, 351-359 (2012).
11. R.M. Sugrue and J. Buongiorno, “A modified force-balance model for predicting bubble departure diameter in subcooled flow boiling”, *15th International Topical Meeting on Nuclear Reactor Thermal-Hydraulics* (*NURETH 15*), Pisa, Italy, 2013.
12. M. Colombo and M. Fairweather, “Prediction of bubble departure in forced convection boiling: A mechanistic model”, *International Journal of Heat and Mass Transfer*, **85**, pp. 135-146 (2015).
13. G.H. Yeoh, S. Vahaji, S.C.P. Cheung and J.Y. Tu, “Modeling subcooled flow boiling in vertical channels at low pressures – Part 2: Evaluation of mechanistic approach”, *International Journal of Heat and Mass Transfer*, **75**, pp. 754-768 (2014).
14. R. Thakrar and S.P. Walker, “CFD prediction of subcooled boiling flow with semi-mechanistic bubble departure diameter modelling”, *25th International Conference Nuclear Energy for New Europe* (*NENE 2016*), Portorož, Slovenia, September 5-8, 2016.
15. CD-adapco, *STAR-CCM+® Version 10.04 User Guide* (2015).
16. G.C. Bartolomei and V.M. Chanturiya, “Experimental study of true void fraction when boiling subcooled water in vertical tubes”, *Thermal Engineering*, **14**, pp. 123-128 (1967).
17. V.I. Tolubinsky and D.M. Kostanchuk, “Vapour bubbles growth rate and heat transfer intensity at subcooled water boiling”, *4th International Heat Transfer Conference*, Paris, France, 1970.
18. G. Kocamustafaogullari, “Pressure dependence of bubble departure diameter for water”, *International Communications in Heat and Mass Transfer*, **10**, pp. 501-509 (1983).
19. G. Garnier, E. Manon and G. Cubizolles, “Local measurements on flow boiling of refrigerant 12 in a vertical tube”, *Multiphase Science and Technology*, **13**, 1-111 (2001).
20. M. Ishii and T. Hibiki, *Thermo-fluid dynamics of two-phase flow*, Springer, New York, USA (2006).
21. A. Tomiyama, I. Kataoka, I. Zun and T. Sakaguchi, “Drag coefficients of single bubbles under normal and micro gravity conditions”, *JSME International Journal Series B Fluids and Thermal Engineering*, **41**, pp. 472-479 (1998).
22. A.D. Burns, T. Frank, I. Hamill and J.M. Shi, “The Favre averaged drag model for turbulent dispersion in Eulerian multi-phase flows”, *5th International Conference on Multiphase Flow*, Yokohama, Japan, 2004.
23. W.P. Jones and B.E. Launder, “The prediction of laminarization with a two-equation model of turbulence”, *International Journal of Heat and Mass Transfer*, **15**, pp. 301-314 (1972).
24. S. Lo and D. Zhang, “Modelling of break-up and coalescence in bubbly two-phase flows”, *Journal of Computational Multiphase Flow*, **1**, pp. 23-38 (2009).
25. M. Colombo and M. Fairweather, “RANS simulation of bubble coalescence and break-up in bubbly two-phase flows”, *Chemical Engineering Science*, **146**, pp. 207-225 (2016).
26. W.E. Ranz and W.M. Marshall, “Evaporation from drops”, *Chemical Engineering Progress*, **48**, pp. 141-146 (1952).
27. T. Hibiki and M. Ishii, “Active nucleation site density in boiling systems”, *International Journal of Heat and Mass Transfer*, **46**, pp. 2587-2601 (2003).
28. H.K. Forster and N. Zuber, “Growth of a vapor bubble in a superheated liquid”, *Journal of Applied Physics*, **25**, pp. 474-478 (1954).
29. B.B. Mikic, W.M. Rohsenow and P. Griffith, “On bubble growth rates”, *International Journal of Heat and Mass Transfer* **13**, pp. 657-666 (1970).
30. L.Z. Zeng, J.F. Klausner, D.M. Bernhard and R. Mei, “A unified model for the prediction of bubble detachment diameters in boiling systems – I. Pool boiling”, *International Journal of Heat and Mass Transfer*, **36**, pp. 2261-2270 (1993).
31. R. Cole, “A photographic study of pool boiling in the region of the critical heat flux”, *AIChE Journal*, **6**, pp. 533-538 (1960).